FAST TRACK COMMUNICATION

Polar multipoles in wurtzite-like crystals (ZnO, GaN)

Stephen W Lovesey[1,2] and Ewald Balcar[3]

[1] ISIS Facility, RAL, Oxfordshire OX11 0QX, UK
[2] Diamond Light Source Ltd, Oxfordshire OX11 0QX, UK
[3] Vienna University of Technology, Atominstitut, Stadionallee 2, A-1020 Vienna, Austria

Abstract
A theoretical analysis and simulation of resonance-enhanced x-ray Bragg diffraction by wurtzite-like crystals is presented for parity-even and polar (parity-odd) atomic resonant processes. Compounds with this crystal structure are of great interest for a range of technologies. The electronic properties of a crystal are represented as ground-state expectation values of atomic multipoles, and the analysis respects all selection rules imposed on diffraction by atomic and crystal symmetry. Our main focus is directed at weak, space-group forbidden reflections that are a result of angular anisotropy in the cation electron distribution. Expected variations of the diffracted intensity with orientation of the crystal due to angular anisotropy of the electron distribution are simulated. The crystal symmetry allows the intensity to be coupled to circular polarization in the primary beam and illustrative examples for the creation of circular polarization in diffraction are provided. These polarization effects are unique probes of electronic structure. Moreover, we prove that recent diffraction experiments on ZnO reveal the pyroelectric (dipole) and polar octupole moment of the cation.

1. Introduction

Wurtzite-like crystals are both pyroelectric and piezoelectric and possess a unique hexad axis of symmetry which is necessarily the direction of the pyroelectric moment (unique in the sense that the hexad axis is not repeated by any symmetry element in the point-group). The non-centrosymmetrical crystal structure, $6mm$, is a member of the polar crystal class and it is not handed (enantiomorphic) or optically active.

Zinc oxide (ZnO, zincite) is a wide-band-gap semiconductor of current interest for a range of applications [1], including, a transparent conductor in solar cells and a material in transparent transistors. Fractional substitution of Zn by Li produces a ferroelectric while substitution by Ni produces a magnetic modification. Zincite emits light in the blue-to-UV range with efficiency superior to that of gallium nitride (GaN). Gallium nitride is a key component of optoelectronic devices working in the blue–violet range, quantum-well structures and nanowires. Cations in ZnO and GaN have the same oxidation state which is a closed shell of electrons ($3d^{10}$). In the ideal wurtzite structure the relative cation–anion bond aligned along the [001] direction has a length 3/8. Reported values

for the relative bond length of ZnO and GaN are, respectively, 0.3819 [2] and 0.3789 [3].

The wurtzite-like structure uses two sets of positions of type 2(b) from the space-group $P6_3mc$ (number 186) with coordinates 1/3, 2/3, z; 2/3, 1/3, $z + 1/2$, and $z = 0$ and $z \simeq 3/8$ for the cation and anion sites, respectively. The screw axis 6_3 is not handed but neutral. At high pressures the wurtzite-like structure of zinc oxide changes to NaCl-like. Many materials with interesting physical properties possess the spatial symmetry of space-group $P6_3mc$, including, ordered hexagonal δ-MoN which is a superconductor with a transition temperature = 12.1 K.

Occupied positions have symmetry $3m$ (C_{3v}) which does not contain inversion symmetry or a sense of hand. Electronic polar multipoles that transform with respect to inversion symmetry as pseudotensors are forbidden in point-group symmetry $3m$ (the pseudotensor of rank zero is a pseudoscalar, e.g., chirality of a molecule or a crystal structure). In consequence, natural circular dichroism is not supported in materials with the wurtzite-like structure because this dichroic signal arises from polar pseudotensors, with quadrupole character. Absence of natural circular dichroism from the

wurtzite-like structure is usefully contrasted with its absence from paramagnetic modifications of haematite, Cr_2O_3 and V_2O_3. All these compounds form crystals with a rhombohedral corundum structure that belongs to the centrosymmetrical crystal class D_{3d} in which natural circular dichroism is forbidden by symmetry in the crystal class. Metal ions in the corundum structure occupy sites with enantiomorphic (chiral) symmetry 3 (C_3) that allow polar multipoles which transform as pseudotensors to be different from zero. As we already mentioned, natural circular dichroism arising from polar, quadrupole pseudotensors is forbidden for D_{3d} symmetry yet these very same pseudotensors contribute in resonant x-ray Bragg diffraction a class of chirality-induced space-group forbidden reflections [4, 5].

In wurtzite-like structures atomic polar multipoles that transform as true tensors may contribute in resonant x-ray Bragg diffraction. The tensors in question have an odd rank, K, with, for example, $K = 1$ (dipole) and $K = 3$ (octupole). The dipole is associated with the pyroelectric moment, of course. Such contributions to x-ray diffraction by ZnO have recently been investigated by Goulon *et al* [6]. The primary x-ray energy, E, matched the Zn K-absorption edge ($E = 9675$ eV) and the intensity of the space-group allowed (3, 0, 0) reflection was measured as a function of the orientation of the crystal about the Bragg wavevector. In addition to this type of reflection, we investigate theoretically intensity expected from space-group forbidden reflections $(3n, 0, l)$ and (h, h, l) with integer Miller indices and odd l. Interest in these reflections stems from our demonstration that they are caused by the polar octupole and the parity-even hexadecapole ($K = 4$) with the added feature of a direct coupling to circular polarization in the primary x-rays and creation of circular polarization in the secondary beam.

Previously, reflections $(0, 0, l)$ with odd l for a screw axis 6_3 have been theoretically investigated by Dmitrienko [7]. He concluded that these reflections are forbidden if excitation is only by the dipole process, E1–E1. We additionally include processes which are parity-odd (E1–M1 and E1–E2) and parity-even (E2–E2) and with the higher-order processes we find that reflections $(0, 0, l)$ with odd l are allowed.

2. Atomic multipoles

Environments for the two positions 2(b) in $P6_3mc$ are related by a screw axis 2_1 at the point $0, 0, z$ or, alternatively, an axial glide at x, x, z. For a reference site we use $1/3, 2/3, 0$. Local orthonormal axes at this site are taken to be parallel to the reciprocal lattice vector a^* and hexagonal unit-cell axes b_h and c_h. In the space-group $P6_3mc$ mirror planes of symmetry contain the c-axis and they are normal to a_h, b_h and $a_h + b_h$, and so one of our chosen orthonormal axes, b_h, is normal to a mirror.

In our investigation, we follow notation used by Lovesey *et al* [8] and Collins *et al* [9]. Parity-even and polar (parity-odd) atomic multipoles of a cation at our reference site are labelled $\langle T_Q^K \rangle$ and $\langle U_Q^K \rangle$, respectively. Angular brackets $\langle \cdots \rangle$ denote the ground-state expectation value of the enclosed operator and the projection Q satisfies $-K \leqslant Q \leqslant K$. The

triad axis of rotation symmetry parallel to the c-axis in the point-group symmetry of sites 2(b) restricts Q to the values $\pm 3n$. In order to satisfy the mirror plane of symmetry normal b_h atomic multipoles must satisfy,

$$\langle T_Q^K \rangle = (-1)^{K+Q} \langle T_{-Q}^K \rangle = (-1)^K \langle T_Q^K \rangle^* \qquad (1)$$

and

$$\langle U_Q^K \rangle = -(-1)^{K+Q} \langle U_{-Q}^K \rangle = -(-1)^K \langle U_Q^K \rangle^*, \qquad (2)$$

where the additional minus sign in (2) arises because $\langle U_Q^K \rangle$ changes sign under inversion. From (2) we see that $\langle U_0^K \rangle = 0$ for even K, which is a result previously mentioned. Parity-even multipoles with even (odd) K are purely real (imaginary) and vice versa for parity-odd multipoles. Parity-odd multipoles are allowed if the resonant ion is not at a centre of inversion symmetry and here they represent either E1–M1 or E1–E2 resonant events.

3. Unit-cell structure factors

Unit-cell structure factors for ions at positions 2(b) are generated from,

$$\Psi_Q^{K,t} = \left[1 + (-1)^{l+Q} e^{2\pi i(h-k)/3} \right] \langle T_Q^K \rangle, \qquad (3)$$

and

$$\Psi_Q^{K,u} = \left[1 + (-1)^{l+Q} e^{2\pi i(h-k)/3} \right] \langle U_Q^K \rangle. \qquad (4)$$

In these expressions the phase factor $(-1)^Q$ arises from a relative rotation between the two environments for cations of π about the c-axis. The structure factors (3) and (4) share a common factor because the space-group does not contain the inversion operator which distinguishes a parity-even from a parity-odd event. Space-group allowed reflections are indexed by Miller indices for which (3) with $Q = 0$ is different from zero and they include reflections $(3n, 0, 2m)$ and $(h, h, 2n)$.

In the case of $(3, 0, 0)$ our calculated structure factors are consistent with expressions used by Goulon *et al* [6]. Additionally, we provide an interpretation in terms of atomic multipoles of the three parameters in their structure factors. Since (3) and (4) can be different from zero only if $l + Q$ is even, all multipoles have projection $Q = 0$ and the multipoles in question are purely real. For the E1–E1 event unit-cell structure factors are written in terms of,

$$d_{11} = -\frac{2}{\sqrt{3}} \left(\langle T_0^0 \rangle + \frac{1}{\sqrt{2}} \langle T_0^2 \rangle \right), \qquad (5)$$

and

$$d_{33} = \frac{2}{\sqrt{3}} \left(-\langle T_0^0 \rangle + \sqrt{2} \langle T_0^2 \rangle \right). \qquad (6)$$

The tensor of rank zero is proportional to the number of holes in the p-like valence state, and such a term is not present in space-group forbidden amplitudes. In Cartesian coordinates, the quadrupole in (5) and (6) has $(3z^2 - r^2)$ angular symmetry.

Turning to the parity-odd structure factor there is but one parameter, t_{113}, and it is pivotal to an investigation of ZnO made by Goulon *et al* [6]. Their extensive discussion of the

physical properties of t_{113} uses in part an erroneous theory of the E1–E2 event by Marri and Carra [10]. The contribution to the diffracted intensity proportional to circular polarization in the primary beam has a term linear in t_{113} and in measured intensities the term is identified by its dependence on the orientation of the crystal. We find that the parameter is the sum of two true multipoles, namely,

$$t_{113} = 2\left(-\sqrt{3}\langle U_0^1\rangle + \sqrt{2}\langle U_0^3\rangle\right). \tag{7}$$

The dipole in (7) is related to the pyroelectric moment parallel to the c-axis and the octupole has angular symmetry $z(5z^2 - 3r^2)$. Operator equivalents for the dipole and octupole operators are, respectively, a polar unit vector, **n**, and a tensor product $(\mathbf{L} \otimes (\mathbf{L} \otimes \mathbf{n})^2)^3$ where **L** is the operator for angular momentum [8, 10]. An octupole is absent in the E1–M1 event since the triangle rule for coupling two dipoles produces tensors of rank $K = 0, 1$ and 2 and, of course, E1–M1 multipoles of even rank are forbidden in $3m$ symmetry.

4. Space-group forbidden reflections

For the remainder we discuss space-group forbidden reflections with Miller index l an odd integer. One anticipates that such reflections have weak intensity. Optimism about their visibility can be drawn from successful measurements of weak reflections in several other compounds. Specifically, Collins *et al* [11] report resonant diffraction at $(1, 1, 3)$ and $(1, 1, 5)$ reflections from ZnO.

By referring to (3) and (4) one sees that reflections $(3n, 0, l)$ and (h, h, l) with odd l can be different from zero for odd values of the projection, namely, $Q = \pm 3$, and this selection rule means contributions to diffraction can arise from multipoles with rank $K \geqslant 3$. Parity-even tensors have even K in the absence of magnetic order which break time-reversal invariance. Thus there is one multipole, $K = 4$, which contributes to diffraction in the E2–E2 channel. Multipoles in the parity-odd channel E1–E2 stop at $K = 3$.

When the Bragg wavevector is parallel to the c-axis diffraction occurs only through the E2–E2 event and the channel with rotated polarization. We label polarization normal and parallel to the plane of scattering by σ and π, respectively. The unit-cell structure factor for $(0, 0, l)$ with odd l and an E2–E2 event is found to be purely real, and it is,

$$F_{\pi'\sigma} = F_{\sigma'\pi} = \frac{1}{\sqrt{2}}\langle T_{+3}^4\rangle \cos^3\theta \cos(3\psi). \tag{8}$$

Here θ is the Bragg angle, and the angle ψ measures rotation of the crystal about the Bragg wavevector with a^* normal to the plane of scattering at $\psi = 0$. Note the three-fold periodicity in ψ representing in the diffraction amplitude the triad axis of symmetry of the $3m$ symmetry of the site occupied by the resonant ion. The parity-even hexadecapole in (8) has $xz(3y^2 - x^2)$ angular symmetry.

At reflections (h, h, l) with odd l parity-even and parity-odd multipoles both contribute. When the primary σ-polarization, $a^* + b^*$ and c^* lie in the plane normal to the plane of scattering, amplitudes for $\sigma'\sigma$ and $\pi'\pi$ are zero, as we also
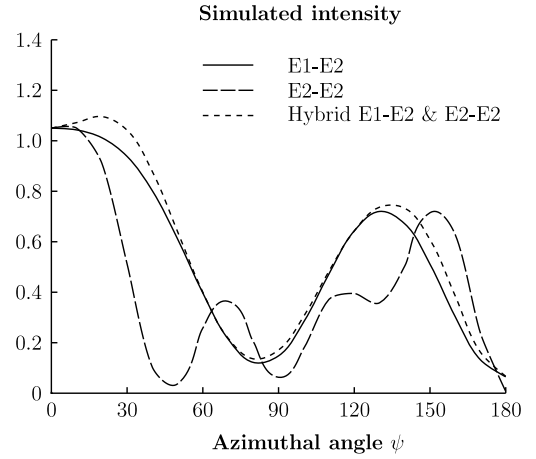
Figure 1. With pure σ polarization in the primary x-rays ($P_3 = +1$) the total diffracted intensity is the sum of intensities in channels with polarization states $\sigma'\sigma$ and $\pi'\sigma$. Simulations of the total intensity for the $(1, 1, 3)$ reflection are given for resonant processes E1–E2, E2–E2 and a mixture of these two processes. In the latter case the resonant energies for E1–E2 and E2–E2 are taken to be different and for the simulation we assume that the resonant energy of E2–E2 exceeds that of E1–E2. The intensity scale in the figure is arbitrary.

find for $(0, 0, l)$. In channels with rotated polarization unit-cell structure factors are,

$$F_{\pi'\sigma} = -F_{\sigma'\pi} = i\sqrt{\tfrac{2}{5}}\langle U_{+3}^3\rangle(\lambda^2 hl/ac), \tag{9}$$

and

$$F_{\pi'\sigma} = -F_{\sigma'\pi} = \frac{1}{\sqrt{2}}\langle T_{+3}^4\rangle(\lambda h/a)\left(3(\lambda l/2c)^2 - 1\right). \tag{10}$$

Note that the structure factors (9) and (10) have a 90° phase difference. A primary energy $E = 9675$ eV corresponds to an x-ray wavelength $\lambda = 1.28$ Å, and cell parameters for ZnO are $a = 3.25$ Å and $c = 5.21$ Å. Expressions (9) and (10) vanish for $h = 0$, and for this value of h expressions (8) and (10) coincide with $\psi = \pi/6$ in (8). At a general setting of the crystal for the observation of reflections (h, h, l) all polarization channels of diffraction can be different from zero.

Figure 1 displays a simulation, using parameters suitable for ZnO, of the total intensity at the reflection $(1, 1, 3)$ for primary linear polarization normal to the plane of scattering. Two simulations use the E1–E2 and E2–E2 processes and a third simulation uses a mixture of these processes. In all reported simulations, the origin of the azimuthal angle, ψ, is chosen such that c^* lies in the plane of scattering. With $\psi = 90°$ all the intensity is in rotated channels of diffraction and (9) and (10) are the corresponding structure factors. Several features of the simulations merit comment. First, the intensity is two-fold periodic and in figure 1 it is displayed in the period $0 \leqslant \psi \leqslant 180°$. Secondly, E1–E2 and E2–E2 intensities as functions of ψ possess individual characteristics that are possibly distinguishable in measured intensities. Finally, a mixture of the two processes, with different resonance energies, is responsible for an intensity distribution unlike that from either process on its own.

At reflections $(3n, 0, l)$ with odd l all four polarization channels can be different from zero with the crystals oriented such that σ, a^* and c^* are contained in the same plane normal to the plane of scattering. Corresponding structure factors for parity-even and parity-odd events differ in phase by $90°$. In consequence, the diffracted intensity is a non-trivial function of circular polarization in the primary beam even when events have exactly the same dependence on the primary energy, which is what we shall assume. Let the diffracted intensity be denoted by $I_0(P_2)$ where P_2 is the helicity in the primary x-ray beam. The difference between intensities recorded with right-and left-handed circular polarizations is found to be,

$$I_0(P_2) - I_0(-P_2) = \frac{2}{\sqrt{5}} P_2 \langle U_{+3}^3 \rangle \langle T_{+3}^4 \rangle \sin(2\theta)$$
$$\times \cos\beta \left(1 - \sin^2\theta \sin^2\beta\right)^2 \qquad (11)$$

with

$$\cos\beta = \frac{2h/\sqrt{3}}{(4h^2/3 + (al/c)^2)^{1/2}}$$

and $\sin\theta \sin\beta = (\lambda l/2c)$. (For the reflection $(3, 0, 1)$ from ZnO the Bragg angle $\theta = 43.9°$ and $\cos\beta = 0.98$.) With these conditions in channels of diffraction circular polarization is created in the secondary beam, which we denote by P_2'. The calculated effect is,

$$I_0 P_2' = \frac{1}{\sqrt{5}} \langle U_{+3}^3 \rangle \langle T_{+3}^4 \rangle \sin(2\theta) \cos\beta (1 - \sin^2\theta \sin^2\beta)$$
$$\times \left[-(1 - \sin^2\theta \sin^2\beta) + P_3(\cos 2\beta - \sin^2\theta \sin^2\beta) \right], \qquad (12)$$

where P_3 is the Stokes parameter for linear polarization, and $P_3 = +1(-1)$ for pure σ (π) polarization. Effects described by (11) and (12) are highly sensitive probes of the cation's electronic state and the electronic information in the effects can not be obtained with any other experimental method.

5. Summary

We have analysed x-ray Bragg diffraction by wurtzite-like crystals with enhancement of the intensity from parity-even and parity-odd atomic resonant processes. The framework for analysis adopted by us represents electronic properties of a crystal in ground-state expectation values of atomic multipoles, and it respects all selection rules imposed on diffraction by atomic and crystal symmetry. One outcome of our work is significant clarification to observations on ZnO [6]. In the main part of this work, attention is given to weak, space-group forbidden reflections that are a result of angular anisotropy in the cation's electron distribution from covalency (the back-transfer of electrons between a cation and surrounding anions) and hybridization created by odd-order contributions in the electrostatic potential. Angular anisotropy in the electron distribution leads to variations of the diffracted intensity with orientation of the crystal and we provide simulations of anticipated effects. The crystal symmetry is such that, the intensity couples to circular polarization in the primary beam and, conversely, circular polarization is created in diffraction, and both effects are illustrated with specific examples. These effects are unique probes of electronic structure.

References

[1] Pearton S J *et al* 2004 *Vac. Sci. Technol.* B **22** 932
[2] Albertsson J, Abrahams S C and Kvick A 1989
    Acta Crystallogr. B **45** 34
[3] Paszkowicz W *et al* 2004 *J. Alloys Compounds* **382** 100
[4] Dmitrienko V E and Ovchinnikova E N 2001 *Acta Crystallogr.*
    A **57** 642
[5] Di Matteo S *et al* 2003 *Phys. Rev. Lett.* **91** 257402
[6] Goulon J *et al* 2007 *J. Phys.: Condens. Matter* **19** 156201
[7] Dmitrienko V E 1983 *Acta Crystallogr.* A **39** 29
    Dmitrienko V E 1984 *Acta Crystallogr.* A **40** 89
[8] Lovesey S W *et al* 2005 *Phys. Rep.* **411** 233
[9] Collins S P *et al* 2007 *J. Phys.: Condens. Matter*
    19 213201
[10] Marri I and Carra P 2004 *Phys. Rev.* B **69** 113101
[11] Collins S P *et al* 2003 *Phys. Rev.* B **68** 064110